NOAA Climate Data Record (CDR) Project:

Generating consistent radiance FCDRs and deep-layer atmospheric temperature TCDRs from the MSU/AMSU/SSU temperature-sounding channels

Year 2 Annual Report

June 2010 – June 2011
NOAA CDR Chief Scientist: **Dr. Jeff Privette**
NOAA CDR Program Manager: **Dr. Jesse Glance**

Principal Investigator:

Cheng-Zhi Zou
NOAA/NESDIS/Center for Satellite Applications and Research
5200 Auth Road, RM 712
Camp Springs, MD 20746
Phone: 301-763-8042 ext 156, Fax: 301-763-8108, email: cheng-zhi.zou@noaa.gov

Co-Investigators:

Sid Boukabara
NOAA/NESDIS/STAR; Phone: 301-763-8136; email: Sid.Boukabara@noaa.gov

Lidia Cucurull
NOAA/NESDIS/STAR; Phone: 301-763-8000; email: Lidia.Cucurull@noaa.gov

Dick Dee
ECMWF, Phone: (+44) 118 949 9352; email: Dick.Dee@ecmwf.int

Qiang Fu
University of Washington; Phone: 206-685-2070; email: qfu@atmos.washington.edu

Thomas Kleespies
NOAA/NESDIS/STAR; Phone: 301-763-8136; email: Thomas.J.Kleespies@noaa.gov

Carl Mears
Remote Sensing Systems; Phone: 707-545-2904; email: mears@sonic.net

John Woollen
NOAA/NWS/NCEP; Phone: 301-763-8000; email: Jack.Woollen@noaa.gov

Table of Contents

Purpose of this Document 2
Project Objectives 2
Summary of Accomplishments 2
MSU radiance FCDRs and atmospheric temperature TCDRs 2
AMSU-A radiance FCDR 3
Merged MSU and AMSU atmospheric temperature TCDR 4
SSU stratospheric temperature TCDR 5
Comparisons between AMSU-A and GPSRO data 6
Comparisons with reanalysis data 7
Reconciling MSU jumps and its impact on tropical tropospheric temperature trend estimate 8
Poleward Shift of Subtropical Jets Inferred from Satellite observations 8
Dataset Availability 9
Publications 9
Selected Meeting Presentations 9
Annual Report from University of Washington 11-25

1. Purpose of this Document

This document is a report of activities that took place during the second year of the NOAA Climate Data Record (CDR) project "Generating consistent radiance SDRs and deep-layer atmospheric temperature TCDRs from the MSU/AMSU/SSU temperature-sounding channels". This is a three year project. Four different agencies/institutions are involved: the NOAA/NESDIS/Center for Satellite Applications and Research (STAR) in Camp Springs, MD; the University of Washington (UW) in Seattle, Washington; Remote Sensing Systems (RSS) in Santa Rosa, CA; and European Centre for Medium-Range Weather Forecasts (ECMWF) in Reading, United Kingdom. This report summarizes work done by STAR and UW which receive funding from the CDR program. RSS will report directly to the CDR program manager.

2. Objectives

The primary objective of the project is to develop consistent, inter-calibrated MSU/AMSU/SSU radiance fundamental climate data records (FCDRs) and their subsequent deep-layer atmospheric temperature thematic climate data records (TCDRs). This will include MSU-, AMSU-, and SSU-only radiance FCDRs and temperature TCDRs as well as merged MSU/AMSU and AMSU/SSU temperature TCDRs. The project will extend the NESDIS inter-calibration effort by including more products with extended time period. A second objective of the project is to have the MSU/AMSU/SSU data production teams and climate application community to work closely for an optimal use of the inter-calibrated dataset.

3. Summary of Accomplishments

The accomplishments are segmented into development and merging of FCDRs and TCDRs from different instruments. Application and comparison of the FCDRs and TCDRs with other data sources are also summarized.

3.1 MSU radiance FCDRs and atmospheric temperature TCDRs

MSU-only FCDR and TCDR developments had been described in the annual report for the first project year. No changes were made for these products since then. However, we begin to examine the differences between the model simulated and observation-derived diurnal anomaly datasets and their impacts on the MSU TCDR product. In current available versions of the STAR MSU/AMSU TCDR datasets (Versions 1.2 and 2.0), climate model simulated diurnal anomalies were applied for diurnal drift corrections. However, unrealistic temperature trends were found over the high plateau areas, such as the Andes and Himalaya Mountains, where magnitudes of the model-simulated diurnal anomalies are not good enough to correct diurnal drift errors. We have developed a diurnal anomaly dataset based on historical MSU observations, taking advantage the fact that the long-time satellite drifts made observations from different MSU instruments to cover most of the time in a diurnal cycle for a particular position. Figure 1 shows a comparison between the MSU-derived and CCM3 simulated diurnal anomalies

for a particular month and daytime over the Himalaya high plateau. It shows that the MSU-derived diurnal anomalies have larger magnitudes than CCM3 simulated. Impact studies are being planned to understand how these differences affect MSU/AMSU derived temperature trends over these areas.

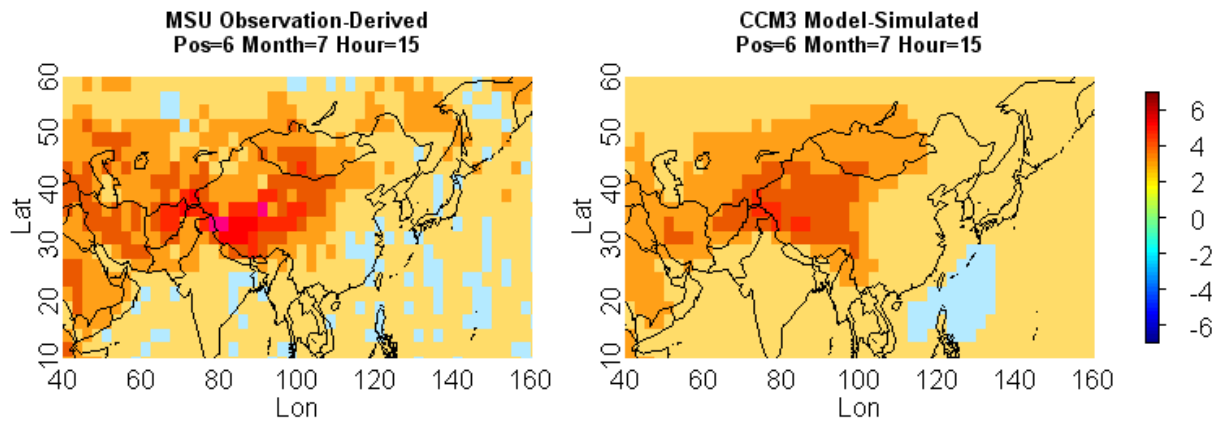

Figure 1 MSU observation-derived versus CCM3 model-simulated monthly mean diurnal anomalies at GMT hour 15 for July (unit in K).

3.2 AMSU-A radiance FCDR

During the first project year, inter-satellite calibration of AMSU-A channels 5 to 10 onboard NOAA-15, -16, -17, -18, and MetOp-A were completed. During the second project year, inter-calibration of channels 12 and 13 for these same satellites were completed. Inter-calibration of AMSU-A channels 11 and 14 has been postponed because NOAA-15 had no data for these two channels since earlier 2000's. Different inter-calibration strategies may need to be developed for these two channels and this will be the task for the third project year.

During the second project year we found an important AMSU-A calibration error--channel frequency drift in certain satellite channels. We also developed a method to determine the actual channel frequency values for such channels. The AMSU-A channel frequency drift issue has not been addressed in previous documentations. In general, radiative transfer models in the numerical weather prediction and reanalysis data assimilation systems adopt channel frequency values from pre-launch measurements to simulate the AMSU observations, based on the belief that those frequency values were the same before and after satellite launch. However, our analysis using simultaneous nadir overpass (SNO) matchups provides evidence that certain satellite channels, such as NOAA-15 channel 6, incurred central frequency shift after satellite launch. Shown in Figure 2 below, scene temperature dependency in the SNO scatter plot between NOAA-18 and NOAA-15 has the shape of 'S' laying on its side. Our analysis indicated that this SNO bias pattern is typically related to the atmospheric lapse rate climatology and thus to the channel frequency shift of one of the satellite in the SNO satellite pairs. Further SNO analysis pointed to NOAA-15 as being the error source. Community Radiative Transfer Model (CRTM) simulation experiments at satellite SNO sites were conducted to determine the actual post-launch channel frequency value of this channel. With the corrected channel frequency

value, the scene temperature-dependent biases in the SNO analysis have been successfully removed (Figure 2b).

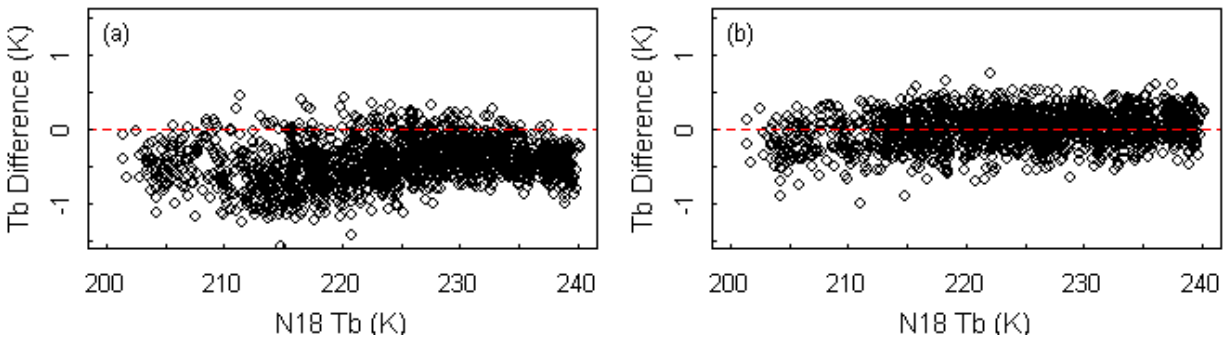

Figure 2 SNO scatter plot for AMSU-A channel 6 brightness temperatures between NOAA-18 and NOAA-15 before (a) and after (b) corrections of the frequency shift in NOAA-15 channel 6. The horizontal and vertical coordinates are respectively the NOAA-18 brightness temperature and the brightness temperature differences between NOAA-15 and NOAA-18 at their SNO sites.

In addition to the channel frequency shift, other calibration errors existing in the operational calibrated AMSU-A level-1c radiance datasets have been identified and minimized (or removed) in our AMSU-A inter-satellite calibration procedure. These include relatively stable inter-satellite biases between most satellite pairs, steady bias drifts on NOAA-16 and channel 7 of MetOp-A, sun-heating induced instrument temperature variability in radiances, and scene temperature dependency in biases due to inaccurate calibration non-linearity. A manuscript describing details of these calibration errors and methods to remove or minimize them has been submitted to *Journal of Geophysical Research* for publication.

3.3 Merged MSU and AMSU atmospheric temperature TCDR

Generation of Version 2.0 of a 33+year (1979-present) merged MSU/AMSU atmospheric temperature TCDR was described in the annual report for the first project year. No major changes were made since then except monthly gridded TCDR dataset became ‘operational’ since July 2010. By ‘operational’, the Version 2.0 monthly MSU/AMSU TCDR is regularly updated during the first week of the current month. Each update adds the monthly-mean, inter-calibrated and multi-satellite merged AMSU-A observations from the last month to the dataset. This allows up-to-date monitoring of the global upper-air temperature changes on a routine basis.

3.4 SSU stratospheric temperature TCDR

Version 1.0, 27-year SSU stratospheric temperature record has been developed and released on STAR’s website during the second project year. This is a major achievement in SSU reprocessing since it provides a well-documented, globally gridded, and well-merged SSU temperature datasets for stratospheric climate change investigations. Reprocessing of the SSU

dataset includes removal or minimization of errors from the following sources: 1) instrument gas leak effect in its CO_2 cell; 2) effect of the atmospheric CO_2 increasing; 3) different observation viewing angles; 4) diurnal sampling biases due to satellite orbital drifts; and 5) statistical merger of SSU observations from different satellites. After reprocessing, the SSU data are composed by nadir-like, gridded brightness temperatures that correspond to identical weighting functions and a fixed local observation time. The global mean anomaly SSU time series for individual satellite after all adjustment procedures are shown in Figure 3. The overall performance of the calibration algorithm is satisfactory in terms of inter-satellite bias removal, except for NOAA-7 channel 2 observations due to missing CO_2 cell pressure vales. The SSU data record comprises global monthly and pentad layer temperatures, with grid resolution of 2.5^0 latitudes by 2.5^0 longitudes, of the mid-stratosphere (TMS), upper-stratosphere (TUS), and top-stratosphere (TTS), which correspond to the three SSU channel observations. For 1979-2006, the global mean trends for TMS, TUS, and TTS, are respectively -1.236±0.131, -0.912±0.145, and -1.006±0.194 K/decade.

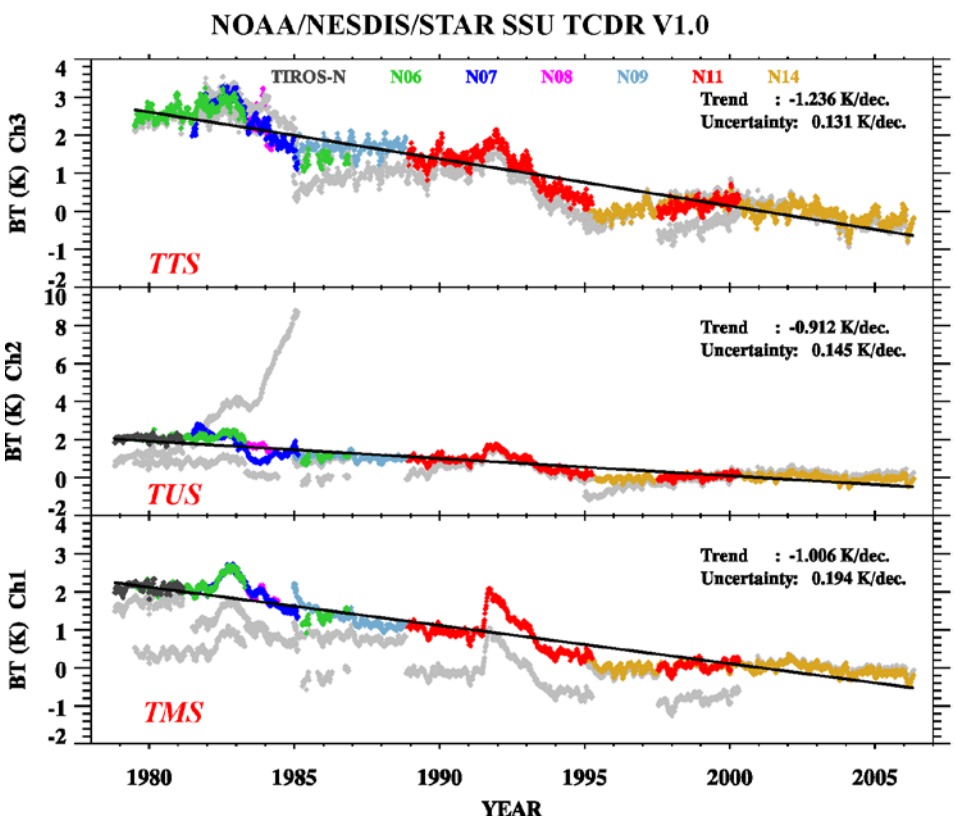

Figure 3 Global mean SSU anomaly time series for individual satellite before (light grey) and after (color) corrections of all related error sources.

Spatial trend distributions for TMS, TUS, and TTS are shown in Figure 4. Consistent trend patterns among the three channels suggest internal consistencies in the processing procedures.

The dataset is freely accessible on the STAR website. A manuscript describing details of the processing and bias correction method has been submitted to *J. Climate* for review and

publication.

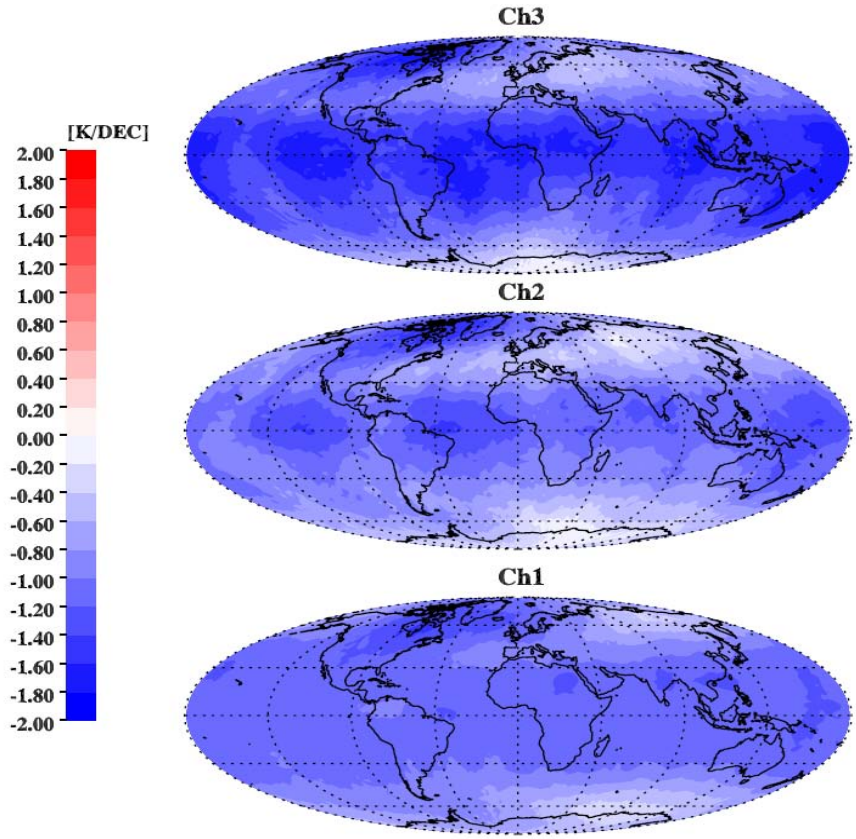

Figure 4 Spatial distributions of linear trends for layer temperature anomalies of mid-stratosphere (ch1, near 10 hPa), upper-stratosphere (ch2, near 5 hPa) and top-stratosphere (ch3, near 1 hPa) during 1978-2006.

3.5 Comparisons Between AMSU-A and GPS-RO Data

GPS-RO temperature data are believed to possess an absolute accuracy of less than 0.2-0.3 K between 5 and 25 km. GPS-RO refractivity from the COSMIC mission is operationally assimilated into the ECMWF and NCEP global data assimilation systems as well as NCEP CFSR reanalysis system. Furthermore, no bias correction is made for the GPS-RO data before they are assimilated. Thus GPS-RO data are used as an anchor in NWP and reanalysis data assimilations. It is desirable to understand the absolute accuracies of the inter-calibrated AMSU-A data by comparing them with GPS-RO observations.

Figure 5 compares the GPS-RO COSMIC retrievals with the AMSU-A channel 9 brightness temperatures derived from the SNO inter-calibration and the operational calibration for a randomly selected time period, July 2007. The comparisons are divided into three regions: Arctic (60^0N-90^0N, red dots), Antarctic (60^0S-90^0S, blue dots), and the rest of the Earth (60^0N-60^0S, green dots). Only the near nadir (the 15th footprint) comparison is provided, but limb

comparisons show similar results. As shown, the mean differences between the SNO calibrated brightness temperatures and COSMIC retrievals are only of 0.01 K, compared to 0.30 K between the operational calibrated AMSU-A data and COSMIC retrievals. This improvement occurs for all three regions. Furthermore, since SNO inter-calibration removes inter-satellite biases, other SNO inter-calibrated satellites show accuracies (relative to GPS-RO) similar to NOAA-15. For example, operational calibrated NOAA-18 channel 9 has a bias about 1 K relative to COSMIC retrievals, but the SNO inter-calibrated NOAA-18 channel 9 has a bias down to the level of 0.1 K (not shown). These statistics are quite encouraging, suggesting that the SNO inter-calibrated data are of higher accuracy than the operational calibrated data.

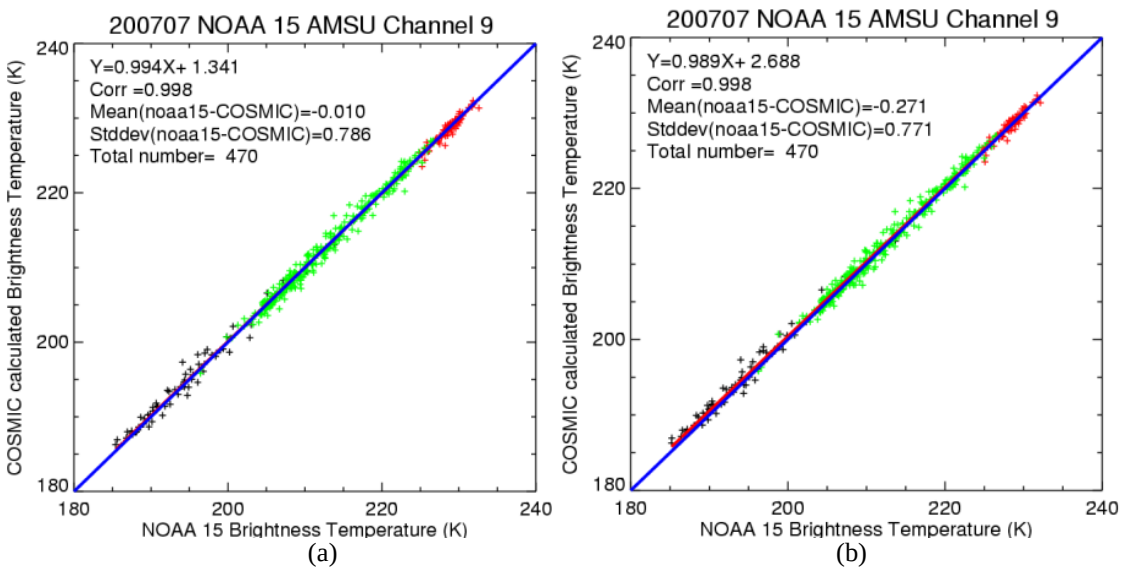

Figure 5 Scatter plot between the AMSU-A channel 9 brightness temperature at the 15th footprint onboard NOAA-15 and the collocated COSMIC retrievals during July 2007. The red dots represent the Arctic (60^0N-90^0N) data, the blue dots the Antarctic (60^0S-90^0S) data, and the green dots for the rest of the Earth (60^0N-60^0S). (a) SNO calibrated brightness temperature versus COSMIC; (b) Operational calibrated brightness temperature versus COSMIC (Plots courtesy of Dr. Wenying He, Institutes of Atmospheric physics, China)

3.6 Comparisons with Reanalysis data

MSU/AMSU radiances are one of the most important data sources for use in climate reanalysis development. These data were bias corrected before being assimilated into reanalysis systems to remove potential biases of individual satellite for them to be consistent with the favorable atmospheric state determined by all input observations. Comparisons between satellite inter-calibration and reanalysis outputs are helpful in identifying the merits or drawbacks in the two different processes in correcting the original MSU/AMSU biases.

Figure 6a shows the ocean-mean brightness temperature anomaly time series of the SNO recalibrated NOAA-15 AMSU-A channel 5 and the ERA-Interim reanalysis mapped into the NOAA-15 observations for the same channel. It is found that the ERA-Interim agrees with the SNO inter-calibrated data reasonably well during 1998-2005; however, the ERA-Interim drifted upward relative to the SNO inter-calibrated data after 2005. Our inter-satellite calibration results

indicate that NOAA-15 channel 5 is a nearly perfect linear channel (Zou and Wang 2011). For this channel, pre-launch calibrated observations are as good as the SNO recalibration for NOAA-15. Furthermore, the SNO inter-calibration resulted in nearly identical observations for all other satellites including NOAA-16, -17, -18, and MetOp-A (Figure 6b). Thus there is no reason to believe that observations from all these nearly identical satellites were drifting to a wrong direction. Therefore, the relative drift between ERA-Interim and SNO inter-calibrated data is believed to be caused by certain changes in the ERA-Interim. This confirms the findings in Dee and Uppala (2009) that spurious warming in the ERA-Interim upper-troposphere occurred and it can be attributed to the assimilation of an increasingly large number of warmly biased aircraft temperatures during the year 2000s.

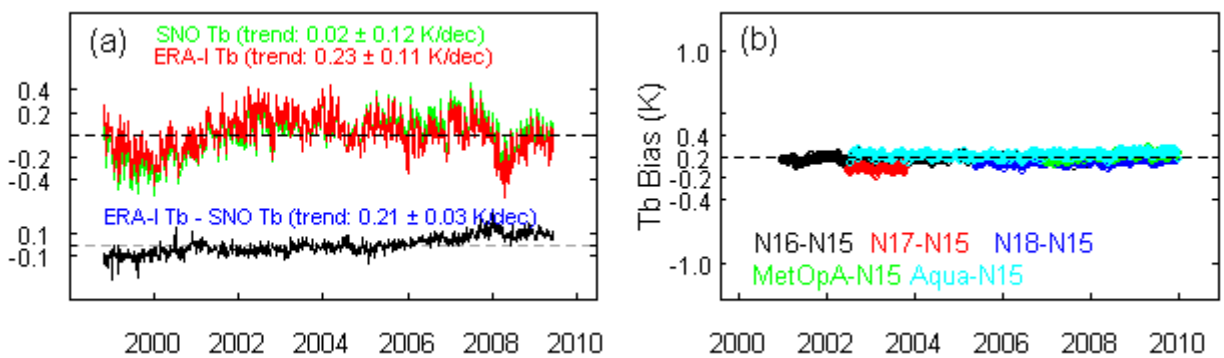

Figure 6 (a) Top trace: Global ocean-mean anomaly time series of the SNO calibrated NOAA-15 T_b (SNO T_b, green) and the ERA-Interim reanalysis mapped into the NOAA-15 observations (ERA-I T_b, red). Bottom trace: differences between the ERA-I T_b and SNO T_b. (b) Inter-satellite brightness temperature difference time series after SNO inter-satellite calibrations.

3.7 Reconciling MSU jumps and its impact on estimates of tropical tropospheric temperature trends

We identified the jumps in difference time series in tropical tropospheric temperatures among the NOAA, RSS, and UAH MSU/AMSU datasets. We examined and corrected these jumps using the radiosonde datasets. It is found that the jumps in 1985-1987 have a large impact on the total trends for 1979-2009. With corrections of these jumps, the tropical tropospheric temperature trends from NOAA, RSS, and UAH are all larger than the surface trends, and the discrepancies in these trends from three MSU/AMSU datasets are reduced.

The details for these findings are described in the following 'Annual Report from the University of Washington', which is part of this combined annual report.

3.8 Poleward Shift of Subtropical Jets Inferred from Satellite observations

One pronounced feature in observed latitudinal dependence of MSU/AMSU T_4 trends is the enhanced cooling near 30° latitude in both hemispheres (Fu et al. 2006). This observed phenomenon has not, to date, been explained in the literature. We show that the enhanced T_4 cooling is a direct response of the lower-stratospheric temperature to the poleward shift of

subtropical jets. Further, this enhanced T_4 cooling can be used to quantify the poleward shift of subtropical jets. Using the MSU/AMSU T_4 from NOAA, RSS, and UAH teams, it is shown that the subtropical jets have shifted poleward by 0.6 ± 0.1 and 1.0 ± 0.3 degrees latitude in the southern and northern hemispheres, respectively, in last 30 years since 1979, indicating a widening of tropical belt by 1.6 ± 0.4 degrees latitude. The tropical widening has important implications regarding changes of regional and global hydrological cycles, climate feedback processes, and our understanding of climate change.

The details for these findings are described in the following 'Annual Report from the University of Washington', which is part of this combined annual report.

4. Dataset Availability

All recalibrated MSU/AMSU/SSU data can be freely acquired through the designated website for the project with the URL address: http://www.orbit.nesdis.noaa.gov/smcd/emb/mscat/mscatmain.htm.

5. Publications

Zou, C.-Z. and W. Wang, 2011, Inter-satellite calibration of AMSU-A observations for weather and climate applications, Submitted to *J. Geophy. Res.*

Wang, L., C.-Z. Zou, H. Qian, 2011: Construction of Stratospheric Temperature Data Records From Stratospheric Sounding Unit, Submitted to *J. Climate*

Zou, C.-Z. and W. Wang, 2010, Stability of the MSU-derived atmospheric temperature trend, *J. Atmos. Oceanic. Technol.*, **27**, 1960-1971.

Zou, C.-Z., M. Gao, M.Goldberg, 2009, Error structure and atmospheric temperature trends in observations from the microwave sounding unit, *J. Climate*, **22**, 1661-1681, DOI: 10.1175/2008JCLI2233.1

Fu, Q., and P. Lin, 2011: Poleward shift of subtropical jets inferred from satellite-observed lower stratospheric temperatures. *J. Climate* (accepted).

6. Selected Meeting Presentations

Zou, C.-Z., 'NOAA Algorithms for Generating MSU/AMSU/SSU Radiance FCDRs and Upper-Air Temperature TCDRs' GSICS Microwave Subgroup Meeting on 10/12/2010

Wang, L., C.-Z. Zou, and H. Qian, 'Newly-Developed NOAA Stratospheric Sounding Unit (SSU) Climate Data Records and Its Climate Applications', *AMS Annual meeting*, Seattle, WA, 01/23/2011-01/27/2011

Zou, C.-Z., ‘An Update on Development of MSU/AMSU/SSU Sounding Channel Radiance FCDR and Upper-Air Temperature TCDR’, STAR CDR workshop, 03/02/2011-03/03/2011

Zou, C.-Z. and W. Wang, ‘DETECTION OF CHANNEL FREQUENCY ERRORS IN POST-LAUNCH CALIBRATION OF AMSU-A OBSERVATIONS’, IGARRS Meeting, Vancouver, Canada, July, 25-29, 2011

Wang, W., and C.-Z. Zou, ‘Lower-Tropospheric Temperature Climate Data Record Using NOAA/NESDIS/STAR Recalibrated MSU/AMSU-A Observations’, IGARRS Meeting, Vancouver, Canada, July, 25-29, 2011

Fu, Q., and C.M. Johanson (invited): Hadley cell widening: Model simulations versus observations. AGU Fall Meeting, December 13-17, 2010, San Francisco, California.

Annual Report to NOAA CDR Program

Project Title: Generating consistent radiance SDRs and deep-layer atmospheric Temperature TCDRs from the MSU/AMSU/SSU temperature-sounding channels

Time Period: June 1, 2010 through June 1, 2011

Science Team Lead: Cheng-Zhi Zou
Center for Satellite Applications and Research (StAR),
NOAA/NESDIS, Camp Springs, MD 20746

Science Team Members: Sid Boukabara, NESDIS/StAR
Lidia Cucurull, NESDIS/StAR
Dick Dee, ECMWF
Qiang Fu, University of Washington
Thomas Kleespies, NESDIS/StAR
Carl Mears, Remote Sensing Systems
John Woollen, NWS/NCEP

Collaborators: Ralph Ferraro/NESDIS/StAR
Ben Ho/UCAR

Report Institute: Department of Atmospheric Sciences
University of Washington, Seattle, Washington

Contributors: S. Po-Chedley, C.M. Johanson, and Q. Fu

Summary

We identified the jumps in difference time series in tropical tropospheric temperatures among the NOAA, RSS, and UAH MSU/AMSU datasets. We examined and corrected these jumps using the radiosonde datasets. Here we focus on the jumps in the period of 1985-1987 when the satellites have little overlaps. Tropical tropospheric temperatures (T_{24}) based on a combination of the MSU/AMSU T_2 and T_4 (Fu et al. 2004; Fu and Johanson 2005) were used, which can be derived from NOAA, RSS, and UAH MSU/AMSU datasets. It is found that the jumps in 1985-1987 have a large impact on the total trends for 1979-2009. With corrections of these jumps, the tropical tropospheric temperature trends from NOAA, RSS, and UAH are all larger than the surface trends, and the discrepancies in these trends from three MSU/AMSU datasets are reduced.

One pronounced feature in observed latitudinal dependence of MSU/AMSU T_4 trends is the enhanced cooling near 30° latitude in both hemispheres (Fu et al. 2006). This observed phenomenon has not, to date, been explained in the literature. We show that the enhanced T_4 cooling is a direct response of the lower-stratospheric temperature to the poleward shift of subtropical jets. Further, this enhanced T_4 cooling can be used to quantify the poleward shift of subtropical jets. Using the MSU/AMSU T_4 from NOAA, RSS, and UAH teams, it is shown that the subtropical jets have shifted poleward by 0.6 ± 0.1 and 1.0 ± 0.3 degrees latitude in the southern and northern hemispheres, respectively, in last 30 years since 1979, indicating a widening of tropical belt by 1.6 ± 0.4 degrees latitude. The tropical widening has important implications regarding changes of regional and global hydrological cycles, climate feedback processes, and our understanding of climate change.

Reconciling the 1987 MSU jump and its impact on estimates of the tropical tropospheric temperature trend

We focus on the tropical troposphere, where there are large discrepancies in MSU/AMSU-derived tropospheric temperature trends from various teams. Current MSU/AMSU T_{24} trends over the tropics (20° S – 20° N) for 1979 – 2009 are 0.070 ± 0.134 K/decade from UAH, 0.144 ± 0.136 K/decade from RSS, and 0.185 ± 0.143 K/decade from NOAA STAR ($p<0.05$). The difference time series trends are 0.039 ± 0.007 K/decade for NOAA-RSS, 0.075 ± 0.012 K/decade for RSS-UAH and 0.114 ± 0.016 K/decade for NOAA-UAH, which are all statistically significant. In addition, tropical tropospheric temperature trends from NOAA and RSS datasets show more warming than the surface, consistent with GCM simulations, while the UAH results show the opposite. Here we report our effort in identifying the jumps in difference time series among various MSU/AMSU datasets and using independent radiosonde data to critically evaluate and correct these jumps. We will focus on assessing the magnitude of the jumps in the period of 1985-1987 when the satellites have little overlaps, which would be useful to help constrain the NOAA-9 target factor and improve the derived tropical tropospheric trend. This effort should also shed light on the relative merit of different inter-satellite merging techniques.

Tropical tropospheric temperatures from satellite MSU/AMSU and radiosode

For this analysis, a linear combination of MSU/AMSU channel 2 and channel 4 are used such that $T_{24} \approx 1.1T_2 - 0.1T_4$ in the tropics (Fu et al., 2004; Johanson and Fu, 2005). This product is a measure of the temperature in the deep troposphere and is favored because it excludes temperature contamination from the stratosphere and can be derived from RSS, NOAA, and UAH datasets (the NOAA team does not currently produce a lower tropospheric T_{2LT} product). As a reference, five radiosonde datasets are used, including RAOBCORE V1.4, HadAT2, IUK, RATPAC-B, and RICH (Haimberger et al., 2008; Thorne et al., 2005; Sherwood et al., 2008; and Free et al., 2005, respectively, RICH is derived using methods from Haimberger et al., 2008, but does not use ERA-40 data). It is important to note that the linear combination of T_2 and T_4 for T_{24} is a physically meaningful measure of the tropospheric temperature as the weighting function above the tropopause is near zero in the tropics.

In creating a synthetic MSU/MSU time series from radiosonde data, monthly radiosonde observations at each pressure level needed to include observations for at least 90% of the time series to be included in the synthetic satellite channel calculation. Further, at least 85% of the weighting function had to be available to calculate a synthetic satellite brightness temperature for a given month. If a radiosonde at a given location had enough observations to calculate a synthetic satellite brightness temperature for 90% of the time series, it was included in the tropical average. If a radiosonde had an observation record sufficiently long for both 00Z and 12Z, these observations were averaged together to create a single time series for each radiosonde location. All individual radiosonde time series were then spatially averaged to create a single tropical tropospheric anomaly series relative to a 1995 to 2005 reference period.

MSU T_{24} observations were co-located with radiosonde observations for each dataset to aid comparison between the two datasets. A spatially averaged tropical tropospheric anomaly time series was then computed from the co-located MSU T_{24} observations. We then computed the difference between the co-located MSU tropical tropospheric temperature series (either NOAA, UAH, or RSS) and the synthetic satellite time series calculated from radiosonde datasets (RICH, RAOBCORE V.1.4, RATPAC-B, IUK, and HadAT2).

Detection of jumps

In order to assess the magnitude of the jumps between the various datasets we applied a number of criteria in identifying breakpoints. The basic breakpoint estimate is defined as:

$$T_B = \sum_{t+1}^{t+k} \frac{T_{diff}(t)}{k} - \sum_{t-k}^{t-1} \frac{T_{diff}(t)}{k} \qquad (1)$$

where T_B is a measure of the magnitude of the break in the time series, $T_{diff}(t)$ is the difference between two different temperature series, and k is an averaging parameter. This expression is simply the difference between the difference time series ahead of and behind a given point, $T_{diff}(t)$. In this analysis, we considered that a breakpoint is significant if:

- The breakpoint was statistically significant ($p<0.05$) using a z-test (taking into account autocorrelation). In particular z needed to exceed 2.58 to reject the null hypothesis. For this statistical test, the null hypothesis is given as:

  H_o: $$\sum_{t+1}^{t+k} \frac{T_{diff}(t)}{k} = \sum_{t-k}^{t-1} \frac{T_{diff}(t)}{k}$$

  and therefore,

  H_1: $$\sum_{t+1}^{t+k} \frac{T_{diff}(t)}{k} \neq \sum_{t-k}^{t-1} \frac{T_{diff}(t)}{k}$$
- Further, we applied a least-squares linear fit and a step function fit centered at t to the region $t-k \le t \le t+k$. We required that the RMS error for the step-function be smaller than the RMS error from the least-squares linear fit in order to avoid spurious breakpoints due to the gradual change.
- In comparing MSU-radiosonde difference series, the breakpoints in the MSU-radiosonde series had to be within one year of a breakpoint in a MSU-MSU difference series. The reason for this requirement is that we are trying to assess the influence of breakpoints between MSU datasets. Although there may be important breaks between MSU and radiosonde datasets, they will not reconcile differences between MSU datasets if they are only present in MSU-radiosonde comparisons. This report focuses on differences between different MSU-derived time series.
- When there are adjacent breakpoints, the breakpoint such that $|T_B|$ is largest is used as the representative breakpoint and the others are disregarded.

We have referred to jumps in the difference series as 'breaks,' 'jumps' and 'breakpoints' – for clarity, breakpoints matching all of the above criteria will be called "break events." Detection of break events in MSU-MSU difference time series is illustrated in Figure 1. Here we use k = 24 months following Christy et al. (2007).

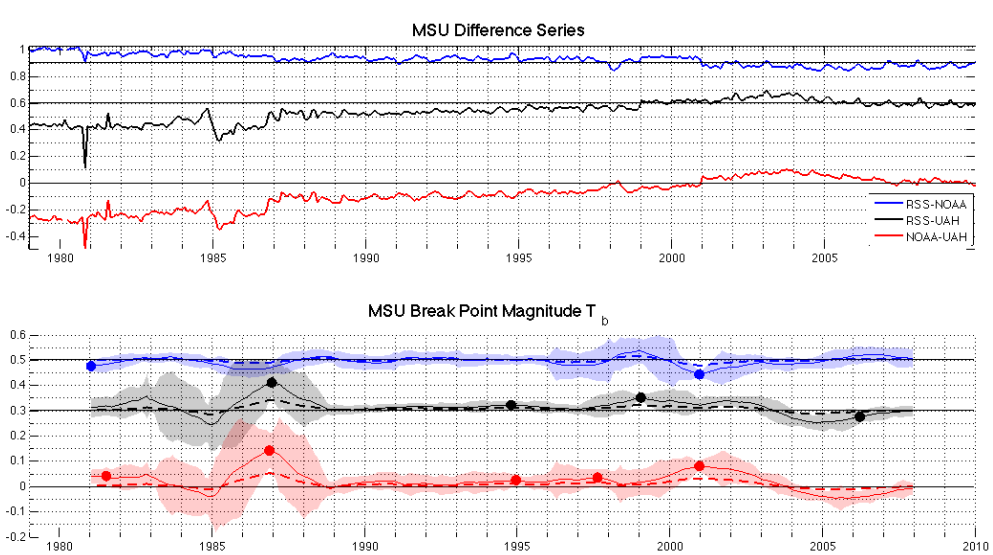

Fig.1. The top panel shows difference time series for RSS, NOAA, and UAH T_{24} over 20°S-20°N. The

bottom panel show the magnitude of the break or jump, T_B, at each point in the difference series (colors legend is the same as the top panel). The shading represents the 95% confidence interval for each break point and the dots represent the detected break events. The dashed line represents the effect the break has on the overall trend. The time series are offset for clarity.

A common problem in breakpoint detection is that breaks that are close to one another can go undetected (as in Haimberger et al., 2008). Since some break events can be less than k months apart, we developed an iterative approach in our breakpoint detection scheme.
It is our hope that we can minimize undetected breaks using this iterative approach. In this analysis, all of the break events in a difference time series are calculated. We then remove the largest break event (i.e. the maximum of $|T_B|$) by applying an adjustment such that:

$$T_{diff-new} = T_{diff}(t) - T_b(t_b) \quad for \quad t \geq t_b \qquad (2)$$

where t_b is the time point for the largest break event. We then repeat this procedure for $T_{diff\text{-}new}$ and continue this iteration until all of the break events are removed. An example of this iterative process is demonstrated in Figure 2; it can be seen that this process brings the difference series between NOAA and UAH trend close to zero. In this example, NOAA is used as a reference time series. In reality, none of the MSU datasets can serve as a reference time series – an independent reference series is needed.

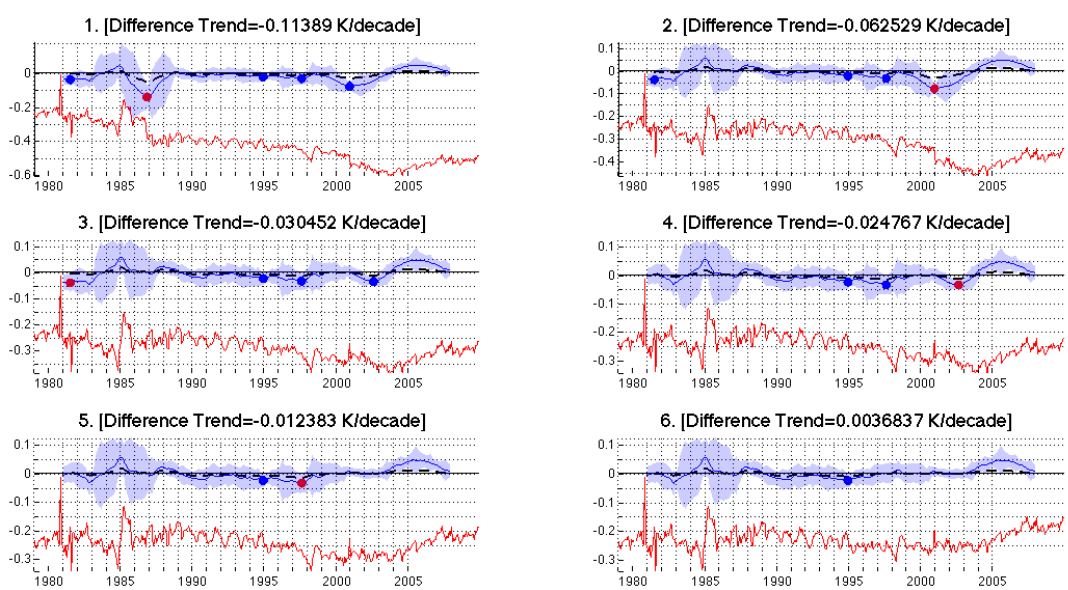

Fig.2. An example of the iterative breakpoint scheme for UAH-NOAA. For each iteration the magnitude of each break is in blue (blue shading represents the 95% confidence interval). The dashed line represents the effect of that particular break point on the overall trend. The red time series represents the difference series at each iteration. The break points are marked with blue dots and the break event at each iteration is marked with a red dot. This break event is then removed in the subsequent iteration.

We begin by using the iterative break event detection to find all the break events common to the MSU T_{24} time series. This process is then applied to each MSU dataset with all of the radiosonde datasets acting as a reference time series. A key assumption made in this analysis is that the radiosonde datasets can serve as a reference over short time periods around MSU breaks.

We have some confidence that this assumption holds, because MSU-radiosonde breaks are typically co-located with MSU jumps (Fig.3). Further, in the tropical mean, it is very unlikely that radiosonde instrument/practice changes would cause jumps at the same time as MSU jumps. Note that we only consider the breaks in MSU/AMSU difference time series and their impacts on their trends. To ensure that radiosondes are pointedly evaluating known MSU jumps, break points for MSU data relative to radiosondes must be co-located (within 12 months) of identified MSU break points. Results for the first iteration of break point identification for each MSU dataset are shown in Figures 3-5.

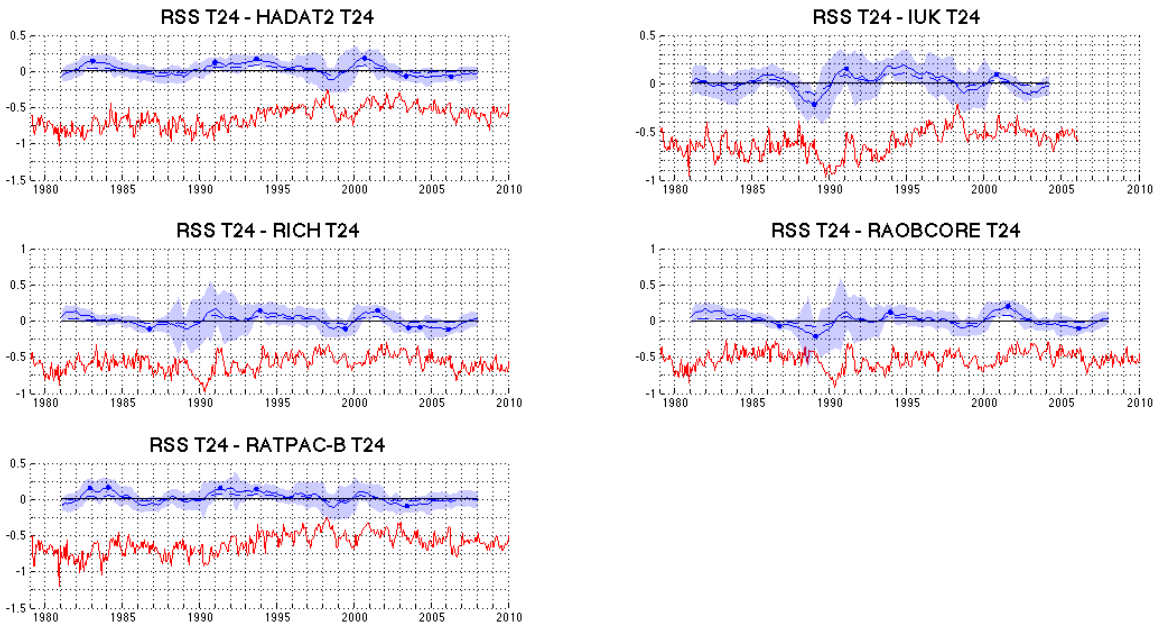

Fig.3. Difference series for RSS relative to different radiosonde datasets (red line). Break point magnitude and 95% confidence interval are represented by the blue line and blue shading. Breaks that are significant and step-like changes are represented with blue dots. Break points in this figure were not required to be located within one year of MSU breaks.

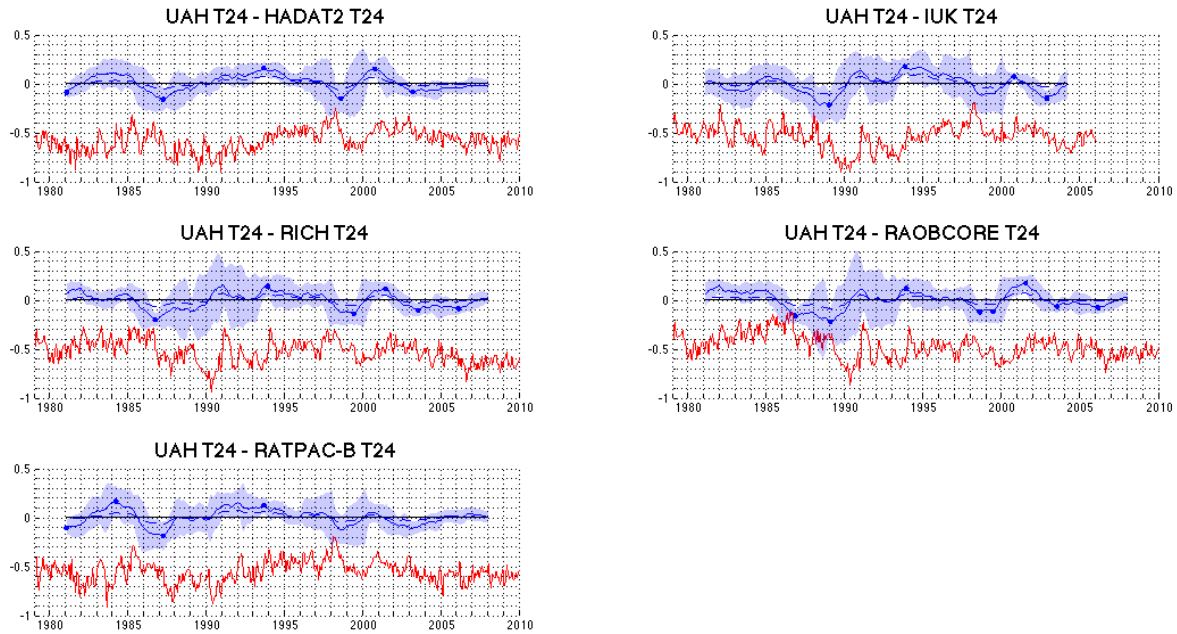

Fig.4. As in Figure 3 but for UAH.

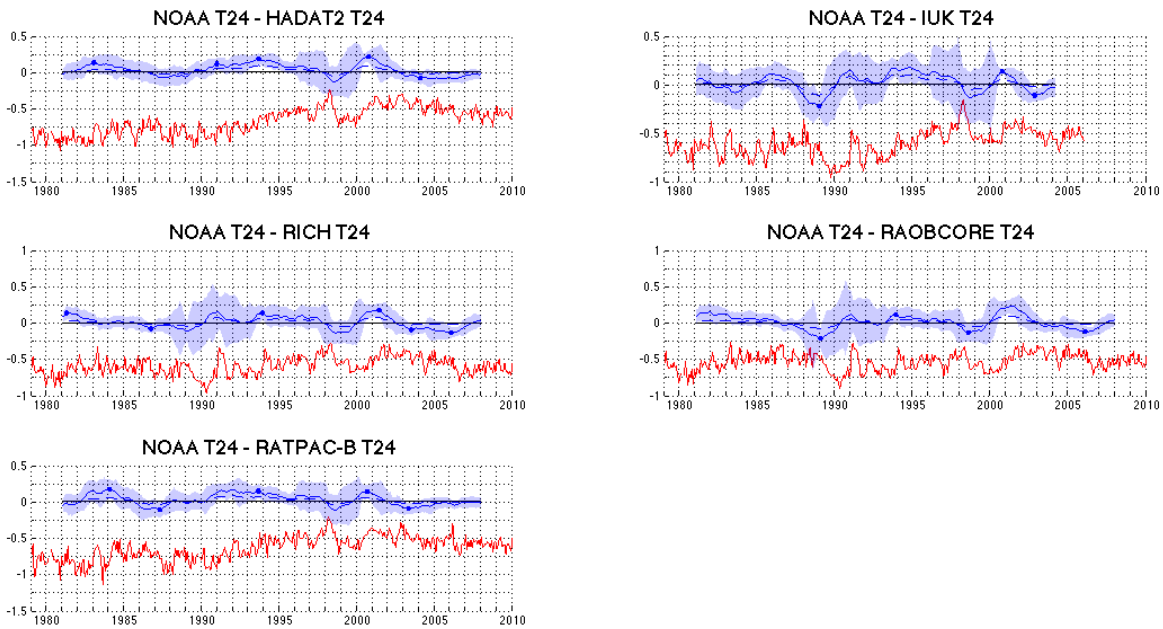

Fig.5. As in Figure 3 but for NOAA.

Figures 3-5 highlights the break points between each MSU dataset and the five radiosonde datasets used in this analysis. While many of the breaks are co-located with known MSU breaks in MSU-only difference series, some breakpoints are not significant in MSU-only comparisons. It is important to note that these breaks could be due to problems with radiosondes

or to a problem common to all the MSU-derived time series. Such problems are outside the scope of this particular work.

Impact of 1987 jumps on MSU/AMSU trends

We present the results for the 1987 jump for an averaging length of 24 months. The results do not change very much for longer averaging periods (i.e. 36 months). The 1985 break point is not significant for the 24 month averaging period. The insignificance of the 1985 break is likely due to the lack of permanence of the jump – the difference nearly returns to the pre-1985 levels by 1986, which suggests that this break does not have a lasting effect on the time series. Christy et al. used averaging periods of 24 and 36 months (but a z-value of 4 and 5, rather than z=2.58 used in this study) (2007).

The effect of the 1987 jump on the trend is presented in Fig. 6. The 1987 jump, relative to radiosonde data, is largest for the UAH dataset no matter what averaging period is used. This indicates that there is likely a problem with the UAH NOAA-9 target factor. The fact that there is a jump at 1987 in the NOAA and RSS datasets relative to radiosonde reference series (albeit smaller) indicates that there may also be problems with the target factors in the RSS and NOAA analysis.

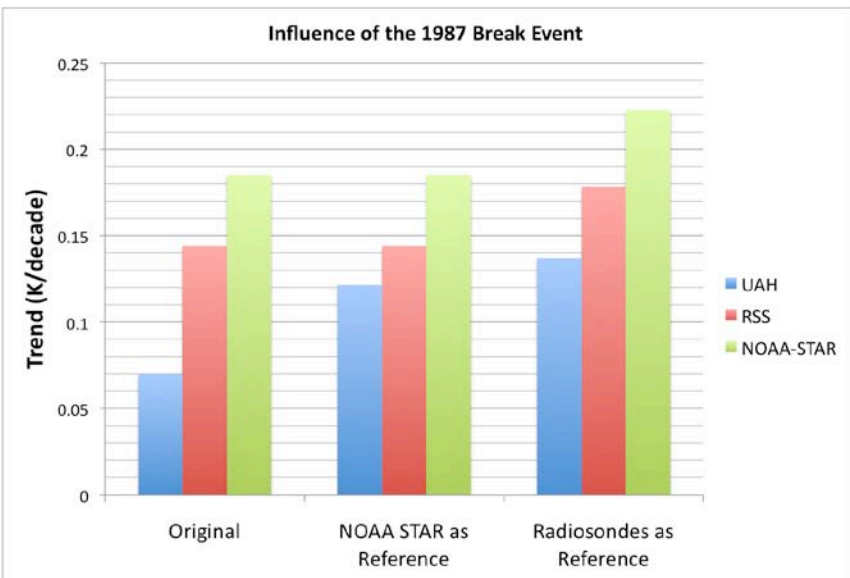

Fig.6. Effect of the 1987 break event on the 20°S – 20°N T_{24} trend using NOAA MSU/AMSU as a reference and radiosondes as a reference for an averaging length of 24 months. RSS does not change using the NOAA reference, because the 1987 break event is not significant between these two groups. Using the radiosondes as a reference assumes that radiosondes do not have a significant jump between 1985 and 1989 (for a 24 month averaging period). While all trends increase with the radiosondes acting as a reference, the trend differences decrease.

Our analysis indicates that the jumps near 1987 associated with various UAH difference series (for both radiosonde and MSU observations) can largely be attributed to UAH. Further,

this step-like change suggests that the UAH NOAA-9 target factor is not optimal. If this problem is corrected, it will likely influence the selection of other target factors and may lead to trend differences larger or smaller than those presented here. The 1985 jump is not considered a break event, since it does not have a long-term impact on the trend.

This work takes initial steps in reconciling differences in tropospheric temperature trends among MSU/AMSU datasets, and we will continue our research effort on this topic in the coming year. Differences between MSU datasets also reveal large breaks near 1999 and 2001, which may have significant impact on the trend estimates. Differences between MSU and radiosonde datasets also suggest disagreement over a breakpoint near 1989, which may be caused by the jumps either in radiosode data or MSU/AMSU data. These breakpoints should also be thoroughly evaluated and corrected. Moreover, most of the datasets show disagreement on a spurious trend throughout most of the 1990s. Spurious gradual changes may also have a large influence on satellite derived temperature trends, so methodology should be developed to evaluate the impact of spurious trends on the overall temperature time series.

Poleward Shift of Subtropical Jets Inferred from Satellite-observed Lower Stratospheric Temperatures

By examining atmospheric temperature trends since 1979 based on satellite-borne microwave sounding unit (MSU) data, Fu et al. (2006) identified the enhanced stratospheric cooling and tropospheric warming in the 15 to 45° latitude belts in both hemispheres. The changes in meridional tropospheric temperature gradients in the vicinity of the jets provide evidence that the subtropical jets have been shifting poleward (Fu et al. 2006). To date, no interpretation has been presented for the enhanced stratospheric cooling. Recently, Ueyama and Wallace (2010) performed an EOF analysis on the MSU lower stratospheric temperatures. They showed that the meridional profile of the second EOF has a bulge at ~30°N/S with the corresponding principal component time series closely mirroring the behavior of the global-mean temperature anomaly (see their Fig. 4). Here we show that the enhanced cooling near ~30°N/S is a direct response of the lower-stratospheric temperature to the poleward shift of subtropical jets.

Because the jet streams mark the poleward limit of the tropical belt, a poleward shift of the jet streams implies a widening of the tropical circulation (Fu et al. 2006). Observational evidence from tropospheric temperatures (Fu et al. 2006), column ozone (Hudson et al. 2006), outgoing longwave radiation (Hu and Fu 2007), and subtropical tropopause heights (Seidel and Randel 2007) collectively indicates that the tropical belt has widened by ~2 to 5° latitude since 1979 (Seidel et al. 2008). Because of the important implication of tropical expansion to the regional and global climate systems (Fu et al. 2006; Seidel et al. 2008), to the cloud-radiation feedback (Norris et al. 2010), and to the test of global climate modeling (Lu et al. 2007; Johanson and Fu 2009), it is critically important to reliably estimate this expansion observationally. In this note, we show that the enhanced lower-stratospheric cooling near 30° latitudes can be employed to quantify the poleward shift of subtropical jets. Using the MSU lower-stratospheric temperature datasets, we find that the subtropical jets have shifted poleward by ~0.6 and ~1.0 degrees latitude in the southern and northern hemispheres, respectively, since 1979, indicating a widening of tropical belt by ~1.6 degrees latitude.

Enhanced lower-stratospheric cooling due to poleward shift of subtropical jets

Figure 7 is a schematic illustration of the poleward shift of subtropical jets and its relation to T_{LS}. The tropopause on the equatorial and poleward side of the jet is at ~100 and 250 hPa levels, respectively (Fig.7a), corresponding to a low and a high tropopause temperature and thus a low and a high temperature in the lower stratosphere (Fig.7b). Therefore, when the jet moves poleward (Fig.7a), the latitudinal dependence of the lower-stratospheric temperature would shift poleward (Fig.7b), which leads to a drop of the lower-stratospheric temperature near the jet latitudes (Fig.7c).

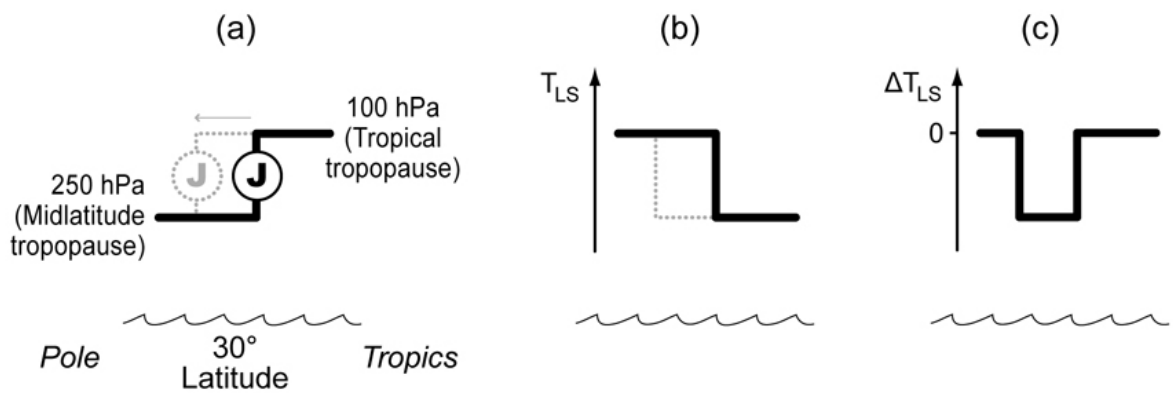

Fig.7. Schematic illustration of the poleward shift of subtropical jets and its impact on the lower-stratospheric temperatures (T_{LS}). (a) Jet positions before and after shift, as shown by solid dark circle with dark J and dashed gray circle with gray J, respectively, along with the arrow indicating the shift direction; (b) latitudinal dependences of T_{LS} before and after jet poleward shift; (c) impact of jet poleward shift on T_{LS}.

The subtropical jets are located at ~200 hPa. Below (above) this level, the temperature decreases (increases) with latitude because of the thermal wind balance (Holton 1992). Thus the smaller T_{LS} within the tropics than that outside is consistent with thermal wind balance associated with the subtropical jets.

The latitudinal profile of the annual-mean T_{LS} from observations is shown in Fig. 8a, which has the smallest value of ~204 K within the deep tropics. It increases with latitude up to about 58°N/51°S, and then decreases toward the poles. The more pronounced polar minimum in the Southern hemisphere (SH) may be related to the weaker Brewer-Dobson circulation in the SH, resulting in less descent and consequently less adiabatic warming over the southern polar cap region (Ueyama and Wallace 2010). It may also be partly caused by the radiative cooling related to the ozone hole there in recent decades.

Figure 8b shows the T_{LS} changes (ΔT_{LS}) corresponding to a poleward shift of the T_{LS} latitudinal profile between equator and 58°N/51°S (i.e., the shaded region in Fig. 8a) by 0.2, 0.4, …, 2.0^o latitudes. Mathematically $\Delta T_{LS} = T_{LS}(L-\Delta L) - T_{LS}(L)$ where L and ΔL are the latitude and change the latitude, respectively. ΔT_{LS} presents a bell-shaped cooling in the subtropics. The cooling is stronger for a larger shift. By defining y as the integration of the T_{LS} changes over

latitudes for given shift (i.e., $y = \int_{\phi_0}^{\phi_1} \Delta T_{LS} d\phi$ where ϕ_0 is zero latitude and ϕ_1 is 58°N/51°S), we thus obtain a linear relation between the *y* and the poleward shift *x*, i.e., *y* = *a***x* where *a* is ~14 and 15 for the SH and NH, respectively. For a given poleward shift *x*, there is a maximum cooling *y'* associated with the bell-shaped cooling (Fig.8b). We also find a linear relation between *y'* and *x*, i.e., *y'* = *a'***x* where *a'* is -0.52 and -0.51 for the SH and NH, respectively.

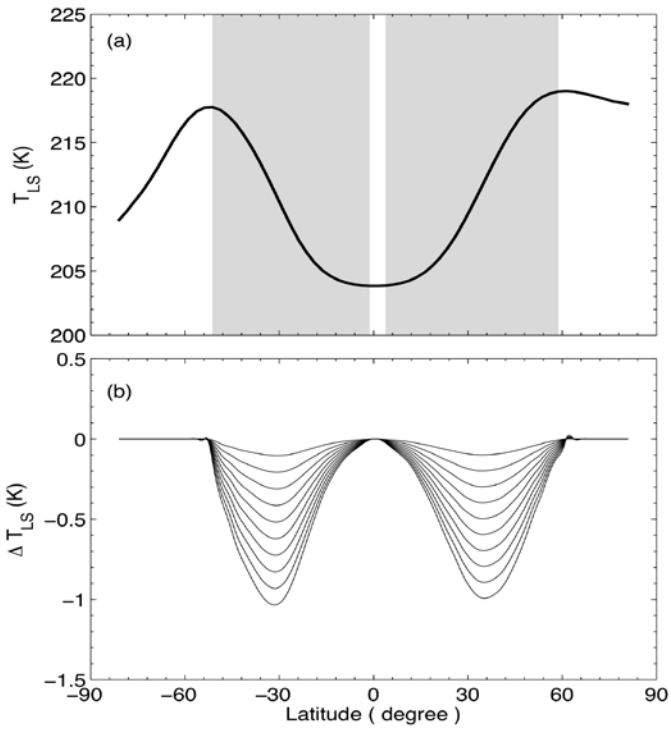

Fig.8. a) Latitudinal profile of climatological (1979-2009) annual-mean T_{LS} based on NOAA MSU dataset; b) T_{LS} changes corresponding to the poleward shift of the shading area in (a) by 0.2, 0.4, 0.6, …, 2.0 degree latitudes.

Herein we interpret the enhanced subtropical cooling in the lower stratosphere as a result of the jet poleward shift (Figs. 7 and 8). We also establish a quantitative relationship between the enhanced cooling and the poleward shift. Therefore we can estimate the poleward shift of the subtropical jets based on the enhanced subtropical lower-stratospheric cooling based on observations.

Quantification of poleward shift of subtropical jets using MSU T_{LS}

Figure 9 shows the latitudinal distributions of MSU T_{LS} trends for 1979-2009 using the UAH (a), RSS (b), and NOAA (c) datasets. A pronounced feature is the enhanced cooling in the subtropical/mid-latitude regions regardless of the datasets used, which is related to the poleward shift of subtropical jets. The T_{LS} trends in last three decades are also caused by the change of the atmospheric compositions such as the increase of the CO_2, O_3 depletion, and possible long-term change of H_2O (e.g., Ramaswamy et al. 2001), and by the change of the Brewer-Dobson circulation (Fu et al. 2010). The T_{LS} trends may also be affected by the El Chichon (1982) and

Pinatubo (1991) volcanic eruptions. In order to isolate the effect of the jet poleward shift on the T_{LS} trend, we need to remove the background trends resulting from other factors. Noting that the poleward shift has little impact on the T_{LS} trend at the Equator, 51°S, and 58°N (see Fig.8b), the trends at these locations are thus the background trends. By assuming that the background trend between equator and 51°S/58°N is linear with latitude, it can be obtained by linear interpolations of trends between equator and 51°S/58°N. We may then estimate the T_{LS} trend due to the jet poleward shift by subtracting the total trends with the background trends.

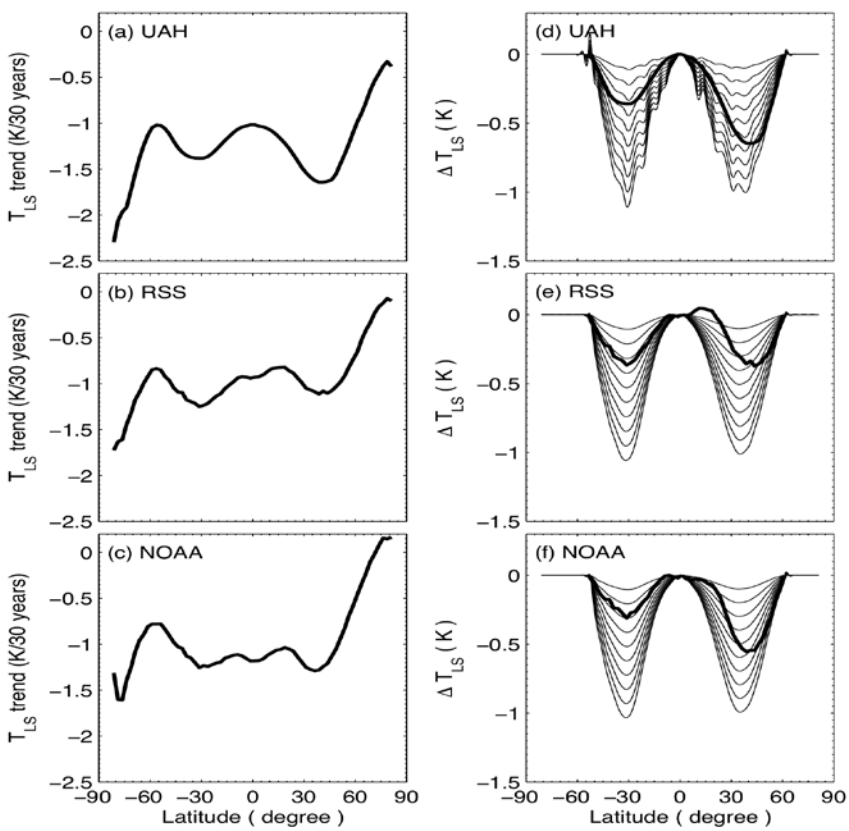

Fig.9. Latitudinal profiles of T_{LS} trends (k/30 years) (a, b, c), and the corresponding contributions due to the subtropical jet poleward shifts (thick lines) (d, e, f) using UAH, RSS, and NOAA MSU datasets, respectively, for 1979-2009. The thin lines in (d, e, f) are the same as those in Fig.2(b) but from three datasets.

The thick lines in Figs. 9 (d,e,f) represent the T_{LS} trend due to the subtropical jet poleward shifts using UAH, RSS, and NOAA MSU datasets, respectively, after removing the background trends. The thin lines in (d, e, f) are the same as those in Fig. 8(b) but from three datasets. We can see that the estimated T_{LS} trend (thick lines) in the SH almost perfectly matches the changes in T_{LS} due to the poleward shift of the latitudinal dependence of the annual mean T_{LS} (thin lines). The comparison of the thick and thin lines indicates a poleward shift of the subtropical jets by about 0.6 to 0.7^o latitude in the SH, depending on the dataset used. In the NH, the thick lines do not match the thin lines as well as in the SH. The comparison of the thick and thin lines in the NH indicates a poleward shift of about 0.8 to 1.3^o latitudes.

We quantify $y = \int_{\phi_0}^{\phi_1} \Delta T_{LS} d\phi$ based on the thick lines in Fig.9 (d,e,f). By employing the *x*-

y relationships from each datasets as derived in section 3, we obtain the poleward shifts of the subtropical jets by 0.7 (UAH), 0.6 (RSS), and 0.5 (NOAA) degree latitudes in the SH, and 1.2 (UAH), 0.7 (RSS), and 1.0 (NOAA) degree latitudes in the NH. We also quantify the maximum cooling *y'* based on the thick lines in Fig.9 (d,e,f). By employing the *x-y'* relationships, we obtain the poleward shifts of the subtropical jets by 0.7 (UAH), 0.6 (RSS), and 0.6 (NOAA) degree latitudes in the SH, and 1.3 (UAH), 0.8 (RSS), and 1.1 (NOAA) degree latitudes in the NH. The results from the two methods agree well with each other and both are also in general agreement with those from a direct comparison of thick and thin lines in Fig.9 (d,e,f). Therefore, the poleward shift of subtropical jets are 0.6 ± 0.1^{o} latitude for SH, and 1.0 ± 0.3^{o} latitude for NH. The errors here are largely caused by the structural uncertainty in various datasets by applying a different set of reasonable processing choices (Thorne *et al*. 2005), but also partly caused by the uncertainty related to the methodology used to derive the widening. It is noteworthy that the observed trends over the NH are lager than over the SH. In contrast, Lu et al. (2007) showed similar trends from each hemisphere based on IPCC AR4 models A2 scenario, while the modeling analysis by Polvani et al. (2011) showed a dominant trend in the SH.

Since the subtropical jets mark the poleward limit of the tropical belt, we obtain a widening of the tropical belt in last thirty years since 1979 by 1.9 (UAH), 1.3 (RSS), and 1.5 (NOAA) degree latitudes using *x-y* relationships, and by 2.0 (UAH), 1.4 (RSS), and 1.7 (NOAA) degree latitudes using *x-y'* relationships . Thus, our estimate of the tropical widening based on MSU T_{LS} datasets is 1.6 ± 0.4^{o} latitude. This result is consistent with the estimate based on the changes in meridional gradients of the tropospheric temperatures using the MSU tropospheric temperature datasets (Fu et al. 2006).

It is noted that we may not be able to fully justify the linearity assumption to remove the T_{LS} background trends. Quantification of the latitudinal dependence of T_{LS} trends due to the changes of the atmospheric composition and large-scale circulations is beyond the scope of the present paper. But it is argued that the linearity assumption may be a good one for the following reasons. First, the remaining trends in the SH after removing the linear background trends almost perfectly matches the shape of the T_{LS} change by shifting climatic T_{LS} poleward (Figs. 9d-f) although in the NH, the thick lines may not match the thin lines as well as in the SH, which may be partly caused by the non-linear latitudinal dependence of the background trends. Second, the latitudinal dependences of T_{LS} trends using three MSU datasets are quite different from each other (Figs. 9a-c) but the remaining trends after removing the background effects agree well (Figs. 9d-f). Third, what we derived is the annual mean trend where the background trend is expected to have less latitudinal structures. We did find that our technique does not work well when applying to various seasons when the background trends may have large latitudinal dependences. It is our future research effort to quantify the uncertainty associated with the non-linear latitudinal dependences of T_{LS} background trends.

The estimate of tropical expansion from this study is at the low end of the range based on various observational analyses (Seidel et al. 2008). But we may have more confidence on the present result for the following reasons. First, many of the other analyses might overestimate the expansion. This is because the threshold values of the total column ozone concentration, outgoing longwave radiation, and tropopause heights that are used to define the tropical belt are

not only affected by the tropical widening, but also by other factors (Davis 2010). For example, both an increase of the tropospheric temperature and a decrease of the stratospheric temperature lead to an increase of the tropopause height (Santer et al. 2003), which is not related to tropical widening. In addition Birner (2010) shows that the widening trend is sensitive to changes in the assumed tropopause height threshold. Note that in the present study, we do not assume a threshold value. More importantly the background trends resulting from factors other than the jet poleward shift are removed before estimating tropical widening. Second, the MSU data used in this study has been scrutinized in much more detail than other observational datasets to satisfy the temporal homogeneity for the trend analysis. More importantly, the use of the shape of remaining temperature trends as a function of latitude, which separates the results from the absolute values of the trends. The latter is more subject to calibration uncertainties in the datasets that occurs due to merging together of many different satellites.

References

Christy, J. R., R. W. Spencer, W. B. Norris, W. D. Braswell, and D. E. Parker, 2003: Error estimates of version 5.0 of MSU-AMSU bulk atmospheric temperatures, *J. Atmos. Oceanic. Technol.*, **20**, 613-629.

Christy, J.R., Norris, W.B., Spencer, R.W. and Hnilo, J.J., 2007, Tropospheric temperature change since 1979 from tropical radiosonde and satellite measurements. *Journal of Geophysical Research*, **112**, p. D06102.

Davis, S. M., 2010: A multi-diagnostic inter-comparison of tropical width time series using meteorological reanalyses and satellite observations, Abstract A33A-0123. *AGU Fall Meeting*, San Francisco, California, Amer. Geophys. Union.

Free, M., Seidel, D.J., Angell, J.K., Lanzante, J., Durre, I. and Peterson, T.C., 2005, Radiosonde Atmospheric Temperature Products for Assessing Climate (RATPAC): a new data set of large area anomaly series. *Journal of Geophysical Research*, **110**, p. D22101.

Fu, Q., Johanson, C.M., Warren, S.G., and Seidel, D.J., 2004: Contribution of Stratospheric Cooling to Satellite-Inferred Tropspheric Temperature Trends . *Nature*, **429**, pp. 55-58.

Fu, Q., and C. M. Johanson, 2005: Satellite-derived vertical dependence of tropical tropospheric temperature trends, *Geophys. Res. Lett.*, **32**, L10703, doi: 10.1029/2004GL022266.

Fu, Q., C. M. Johanson, J. M. Wallace, and T. Reichler, 2006: Enhanced mid-latiude tropospheric warming in satellite measurements, *Science*, **312**, 1179.

Fu, Q., S. Solomon, and P. Lin, 2010: On the seasonal dependence of tropical lower-stratospheric temperature trends, *Atmos. Chem. Phys.*, **10**, 2643-2653.

Haimberger, L., Tavolato, C. and Sperka, S., 2008, Towards elimination of the warm bias in historic radiosonde temperature records – some new results froma comprehensive intercomparison of upper air data. *Journal of Climate*, **21**, pp. 4587 – 4606.

Hu, Y. Y., and Q. Fu, 2007: Observed poleward expansion of the Hadley circulation since 1979, *Atmos. Chem. Phys.*, **7**, 5229-5236.

Hudson, R. D., M. F. Andrade, M. B. Follette, and A. D. Frolov, 2006: The total ozone field separated into meteorological regimes, Part II: Northern Hemisphere mid-latitude total ozone trends. *Atmos. Chem. Phys.*, **6**, 5183–5191.

Johanson, C. M., and Q. Fu, 2009: Hadley cell widening: model simulations versus observations, *J. Climate*, **22**, 2713-2725.

Karl, T. R., S. J. Hassol, C. D. Miller, and W. L. Murray, Eds., 2006: *Temperature trends in the lower atmosphere: Steps for understanding and reconciling differences.* U.S. Climate Change Science Program Synthesis and Assessment Product 1.1, 180 pp.

Lu, J., G. A. Vecchi, and T. Reichler, 2007: Expansion of the Hadley cell under global warming. *Geophysical Research Letters*, **34,** L06805.

Mears, C. A., and F. J. Wentz, 2009: Construction of the remote sensing systems v3.2 atmospheric temperature records from the MSU and AMSU microwave sounders, *J. Atmos. Oceanic. Technol.*, **25**, 1040-1056.

Ramaswamy, V., and Coauthors, 2001: Stratospheric temperature trends: observations and model simulations, *Rev. Geophys.*, **39**, 71-122.

Randall, R.M. and Herman, B.M., 2008, Using limited time period trends as a means to determine attribution of discrepencies in microwave sounding-unit derived tropospheric temperature time series. *Journal of Geophysical Research*, **113**, p. D05105.

Santer, B. D., and Coauthors, 2003: Contributions of anthropogenic and natural forcing to recent tropopause height changes, *Science*, **301**, 479-483.

Seidel, D. J., and W. J. Randel, 2007: Recent widening of the tropical belt: Evidence from tropopause observations. *J. Geophys. Res.*, **112**, D20113, doi:10.1029/2007JD008861.

Seidel, D. J., Q. Fu, W. J. Randel, and T. J. Reichler, 2008: Widening of the tropical belt in a changing climate. *Nat. Geosci.*, **1**, 21–24.

Sherwood, S.C., Meyer, C.L., Allen, R.J., Titchner, H.A., 2008, Robust Tropospheric Warming Revealed by Iteratively Homogenized Radiosonde Data. *Journal of Climate*, **21**, pp. 5336–5352.

Thorne, P. W., D. E. Parker, J.R. Christy, and C.A. Mears, 2005: Uncertainties in climate trends – Lessons from upper-air temperature records. *Bull. Amer. Meteor. Soc*., **86**, 1437-1442.

Thorne, P.W., Parker, D.E., Tett, S.F.B., Jones, P.D., McCarthy, M., Coleman, H., Brohan, P., and Knight, J.R., 2005, Revisiting radiosonde upper-air temperatures from 1958-2002. *Journal of Geophysical Research*, **110**, p. D18105.

Ueyama, R., and J. M. Wallace, 2010: To what extent does high-latitude wave forcing /drive tropical upwelling in the Brewer-Dobson circulation? *J. Climate*, **67**, 1232-1246.

Zou, C.-Z., M. D. Goldberg, Z. Cheng, N. C. Grody, J. T. Sullivan, C. Cao, and D. Tarpley, 2006: Recalibration of microwave sounding unit for climate studies using simultaneous nadir overpasses. *J. Geophys. Res.*, **111**, D19114, doi:10.1029/2005JD006798.

Zou, C.-Z. and Wang, W., 2010, Stability of the MSU-derived atmospheric temperature trend. *Journal of Atmospheric and Oceanic Technology*, **27**, pp. 1960 – 1971.